

Metabolism of MK-0524, a Prostaglandin D₂ Receptor 1 Antagonist, in Microsomes and Hepatocytes from Preclinical Species and Humans

Brian J. Dean, Steve Chang, Maria Victoria Silva Elipe, Yuan-Qing Xia, Matt Braun, Eric Soli, Yuming Zhao, Ronald B. Franklin, and Bindhu Karanam

Department of Drug Metabolism, Merck Research Laboratories, Rahway, New Jersey

Received June 22, 2006; accepted November 16, 2006

ABSTRACT:

(3*R*)-4-(4-Chlorobenzyl)-7-fluoro-5-(methylsulfonyl)-1,2,3,4-tetrahydrocyclopenta[*b*]indol-3-yl acetic acid (MK-0524) is a potent orally active human prostaglandin D₂ receptor 1 antagonist that is currently under development for the prevention of niacin-induced flushing. The major *in vitro* and *in vivo* metabolite of MK-0524 is the acyl glucuronic acid conjugate of the parent compound, M2. To compare metabolism of MK-0524 across preclinical species and humans, studies were undertaken to determine the *in vitro* kinetic parameters (K_m and V_{max}) for the glucuronidation of MK-0524 in Sprague-Dawley rat, beagle dog, cynomolgus monkey, and human liver microsomes, human intestinal microsomes, and in recombinant human UDP glucuronosyltransferases (UGT). A comparison of K_m values indicated that UGT1A9 has the potential to catalyze the glucuronidation of MK-0524 in the liver, whereas UGT1A3 and UGT2B7 have the potential to catalyze the glucuronidation in the

intestine. MK-0524 also was subject to phase I oxidative metabolism; however, the rate was significantly lower than that of glucuronidation. The rate of phase I metabolism was ranked as follows: rat ~ monkey > human intestine > dog > human liver with qualitatively similar metabolite profiles across species. In all the cases, the major metabolites were the monohydroxylated epimers (M1 and M4) and the keto-metabolite, M3. Use of inhibitory monoclonal antibodies and recombinant human cytochromes P450 suggested that CYP3A4 was the major isozyme involved in the oxidative metabolism of MK-0524, with a minor contribution from CYP2C9. The major metabolite in hepatocyte preparations was the acyl glucuronide, M2, with minor amounts of M1, M3, M4, and their corresponding glucuronides. Overall, the *in vivo* metabolism of MK-0524 is expected to proceed via glucuronidation, with minor contributions from oxidative pathways.

Cardiovascular disease, associated with atherosclerosis, is the most common cause of death in the United States. Major risk factors include elevated levels of low-density lipoprotein cholesterol, low levels of high-density lipoprotein cholesterol, and elevated triglyceride levels. Niacin (nicotinic acid) is a member of the vitamin B complex. It is commonly used as a dietary supplement in milligram quantities and as a plasma lipid-modifying drug in gram doses. Niacin increases high-density lipoprotein cholesterol while decreasing plasma concentrations of very low-density lipoprotein and low-density lipoprotein cholesterol (Shepherd et al., 1979; Knoop, 1999). Clinical trials have shown the efficacy of niacin in the management of coronary heart disease when used alone or in combination with other lipid-altering drugs such as statins (Rubenfire, 2004; Zhao et al., 2004).

A major side effect of niacin is the development of cutaneous vasodilation, resulting in flushing of the upper body and face, immediately after dosing (Vogt et al., 2006). Because these effects are

prevalent even at pharmacologically relevant doses, they have limited the widespread use of niacin. Studies have shown that niacin-induced flushing could be reduced by cyclooxygenase inhibitors such as naproxen and indomethacin, suggesting the role of prostaglandins in vasodilation (Eklund et al., 1979; Gentile et al., 1985; Morrow et al., 1992). MK-0524 (Sturino et al., 2006) is a selective antagonist of prostaglandin D₂ receptor 1 (DP1), with an IC₅₀ value of 1.1 nM in a mouse DP1 functional assay (C. Sturino, G. O'Neill, N. Lachance, M. Boyd, C. Berthelette, M. Labelle, L. Li, B. Roy, J. Scheiget, and N. Tsou, unpublished results). MK-0524 has also been shown to block niacin-induced vasodilation in the mouse by ~80% (Cheng et al., 2006). Clinical studies have shown the efficacy of MK-0524 in reducing niacin-induced flushing and is currently under development for this purpose (Cheng et al., 2006). The objective of this study was to delineate the comparative *in vitro* metabolism pathways of MK-0524 using microsomal preparations and hepatocytes isolated from rat, dog, monkey, and humans. Furthermore, studies were also conducted to identify the cytochrome P450 (P450) and UDP glucuronosyltransferase (UGT) isoforms responsible for the *in vitro* metabolism of MK-0524 in humans to aid in designing clinical studies.

Article, publication date, and citation information can be found at <http://dmd.aspetjournals.org>.

doi:10.1124/dmd.106.011551.

ABBREVIATIONS: MK-0524, (3*R*)-4-(4-chlorobenzyl)-7-fluoro-5-(methylsulfonyl)-1,2,3,4-tetrahydrocyclopenta[*b*]indol-3-yl acetic acid; DP1, prostaglandin D₂ receptor 1; P450, cytochrome P450; UGT, UDP-glucuronosyltransferase(s); UDPGA, UDP-glucuronic acid; HPLC, high-performance liquid chromatography; LC/MS/MS, liquid chromatography/tandem mass spectrometry; COSY, correlation spectroscopy; ROESY, rotating frame nuclear Overhauser enhancement spectroscopy.

Materials and Methods

Materials. [Methylsulfonyl- ^{14}C]MK-0524 and its acyl glucuronide (M2) were synthesized by the Labeled Compound Synthesis Group, Department of Drug Metabolism, Merck Research Laboratories (Rahway, NJ). A solution of [^{14}C]MK-0524 was prepared by a 1:10 dilution (v/v) from a stock to yield a solution with a specific activity of 0.12 mCi/mg (243 $\mu\text{g}/\text{ml}$ or 29.2 $\mu\text{Ci}/\text{ml}$). MK-0524 was synthesized by Process Research, Merck Research Laboratories. M1, M2, M3, and M4 standards were obtained from Merck Frosst, Montreal, Canada (Nicoll-Griffith et al., 2006). Recombinant human UGT (UGT1A1, UGT1A3, UGT1A8, UGT1A9, UGT1A10, and UGT2B7) and CYP1A1, CYP2A6, and CYP2E1 were purchased from BD Biosciences (San Jose, CA). Other recombinant human P450s were obtained from the Department of Drug Metabolism, Merck Research Laboratories (West Point, PA). All the P450s contained NADPH-P450 reductase. Sprague-Dawley rat, beagle dog, and rhesus monkey liver microsomes were prepared in-house within the Department of Drug Metabolism, Merck Research Laboratories. Cynomolgus monkey (IVT batch no. M00301-109) and human (IVT batch no. X05841 Lot RDX, mixed gender, $n = 50$) liver microsomes (used only for determination of kinetic parameters for glucuronidation) and beagle dog and human cryopreserved hepatocytes were purchased from Celsis International (Cambridge, UK). Human intestinal microsomes (HJM0040 0402991 SB, from a 42-year-old male subject) were obtained from BD Biosciences. UDP-glucuronic acid (UDPGA), saccharic acid-1,4-lactone, alamethicin, glucose 6-phosphate, NADP $^+$, glucose-6-phosphate dehydrogenase, testosterone, and NADPH were purchased from Sigma-Aldrich (St. Louis, MO). All the solvents were of Optima grade obtained from Fisher Scientific (Pittsburgh, PA). Sprague-Dawley rat and rhesus monkey hepatocytes were prepared in-house following standard isolation protocols.

Kinetics of Glucuronidation of MK-0524. All the reactions were performed in polystyrene 96-well plates (Costar, Cambridge, MA). MK-0524 (25 mM, dissolved in 75% aqueous acetonitrile) was serially diluted to make 12 working standard solutions. The reaction mixture (200 μl) consisted of the substrate, MK-0524 (0.3–625 μM), 50 mM 1,3-Bis[tris(hydroxymethyl)methylamino]propane buffer, pH 7.1, 10 mM MgCl_2 , 10 mM saccharic acid-1,4-lactone, alamethicin (1 $\mu\text{g}/10 \mu\text{g}$ protein), and liver and intestinal microsomes or membrane preparations of recombinant UGT (5–20 μg protein). The reaction mixtures were preincubated for 15 min at 37°C with mixing on a Boekel “Jitterbug” incubator, and the reactions were initiated by the addition of 2 mM UDPGA. Reactions were quenched at 0, 10, 30, or 90 min with 20 μl of 50% acetic acid, followed by 100 μl of acetonitrile. Samples were spun in a centrifuge to remove particulate matter before high-performance liquid chromatography (HPLC) analysis. For K_m and V_{max} determinations, substrate turnover was maintained to approximately 20% to ensure linear conditions for metabolism. Because of the poor aqueous solubility of the compound (0.06 mg/ml, internal Merck document), a visual check was performed on all the samples (UV clear plates). Only data from samples analyzed by HPLC, determined to be in solution (final concentrations up to 40 μM), were used for kinetic determinations.

NADPH-Dependent Phase I Metabolism. Phase I metabolism of [^{14}C]MK-0524 (5 μM) was studied in Sprague-Dawley rat, beagle dog, rhesus monkey, and human liver microsomes. Incubations consisted of microsomes (2 mg protein/ml) suspended in 100 mM potassium phosphate buffer (pH 7.4) and 10 mM MgCl_2 . The reactions were initiated by the addition of an NADPH-regenerating system consisting of 1 mM NADP $^+$, 10 mM glucose 6-phosphate, and 0.7 units/ml glucose-6-phosphate dehydrogenase. Reactions were carried out for 30 or 60 min at 37°C and stopped at appropriate time points by adding half the volume of acetonitrile containing 2% aqueous formic acid. After vortex-mixing and spinning in a centrifuge (14,000 rpm for 10 min), supernatants were analyzed by liquid chromatography/tandem mass spectrometry (LC/MS/MS) with on-line radiometric detection (Beta RAM; IN/US, Tampa, FL). Kinetic experiments with MK-0524 were performed under linear microsomal protein and incubation time conditions in a 96-well format as described above.

Combined Phase I and II Metabolism. To study the in vitro metabolism of MK-0524 under combined phase I and II conditions (rhesus monkey liver microsomes only), 2 mg protein/ml microsomal protein was suspended in 100 mM potassium phosphate buffer, pH 7.4, and 10 mM MgCl_2 was preincubated

in the presence of 0.1 mg/ml alamethicin for 15 min. After the preincubation period, [^{14}C]MK-0524 (5 μM) was added to the microsomal mixture, along with 5 mM saccharic acid-1,4-lactone, an inhibitor of β -glucuronidase, and incubated for a further 5 min at 37°C. The reactions were initiated by the addition of 5 mM UDPGA and an NADPH-regenerating system consisting of 1 mM NADP, 10 mM glucose 6-phosphate, and 0.7 unit/ml glucose-6-phosphate dehydrogenase. The sample mixture was incubated for 15 or 30 min at 37°C. Reactions were stopped by adding half the volume of acetonitrile containing 2% aqueous formic acid to stabilize the acyl glucuronide(s). Samples were vortex-mixed and spun in a centrifuge (14,000 rpm for 10 min at room temperature). The supernatants were analyzed by LC/MS/MS and an on-line radiometric detector (Beta RAM). For NMR analysis of M6, scaled-up incubations of [^{14}C]MK-0524 with monkey liver microsomes in the presence of NADPH and UDPGA were set up as above. Samples were analyzed by HPLC on an SB-Phenyl column as described under *Bioanalytical Methods*. Radioactive peaks corresponding to the peak for M6 were collected based on radioactivity, evaporated to dryness under nitrogen, and reconstituted in acetonitrile/water (50:50, v/v). After HPLC reanalysis on a pristine column under similar conditions as above, the pooled fractions were concentrated under nitrogen and subjected to LC/MS/MS and NMR analysis.

P450 Isoform Determination. All the reactions were performed in 96-well plate format with duplicate time points. The final 200 μl of reaction contained substrate (10 μM), 100 mM potassium phosphate (pH 7.4), 10 mM MgCl_2 , and recombinant P450 microsomes (20 pmol of P450 protein). Reaction mixtures were preincubated for 15 min at 37°C, with mixing on a Boekel “Jitterbug” incubator and reactions initiated by the addition of 1 mM NADPH. Reactions were quenched after 0, 15, 30, or 90 min with 20 μl of 50% aqueous acetic acid followed by 100 μl of acetonitrile. Samples were spun in a centrifuge (14,000 rpm for 10 min at room temperature) before HPLC analysis. To determine the effect of anti-P450 monoclonal antibodies on the reaction, incubations were conducted in the presence of 2.5, 5, 10, or 20 μl of inhibitory CYP3A4 or CYP2C8/9 antibodies or 40 μl of a CYP3A4 and CYP2C8/9 mixture.

Metabolism in Hepatocytes. [^{14}C]MK-0524 (10 μM) was incubated with a suspension of freshly isolated Sprague-Dawley rat and rhesus monkey hepatocytes and cryopreserved beagle dog and human hepatocytes (1×10^6 cells/ml) in a hepatocyte incubation media (IVT, Baltimore, MD) for 0, 60, 120, or 240 min at 37°C under an atmosphere of 95% $\text{O}_2/5\% \text{CO}_2$. Reactions were stopped by adding half the volume of acetonitrile containing 2% aqueous formic acid. Samples were frozen (-70°C for 1 h) and allowed to thaw at room temperature. After vortex-mixing and spinning in a centrifuge (14,000 rpm for 10 min at room temperature), the supernatants were analyzed by LC/MS/MS with on-line radiometric detection (Beta RAM). To isolate M2 and M8 for NMR analyses, scaled-up incubations were conducted with the parent compound and monkey hepatocyte suspensions as described above. Sample analysis was as described for the isolation of M3 from monkey microsomal incubations.

NMR Analysis. NMR analysis was carried out on M3 (a synthetic standard) and M6 (~24 μg based on radioactivity) isolated from an incubation of [^{14}C]MK-0524 with monkey liver microsomes in the presence of NADPH and UDPGA. The spectra were recorded in deuterated acetonitrile (CD_3CN)/deuterated water (D_2O) (2:3, v/v) in 0.15 ml at 25°C (298 K) in 3-mm NMR tubes (Nalorac 3-mm indirect detection gradient probe) and run at 600 and 150 MHz for ^1H and ^{13}C , respectively, using a Varian Unity Inova 600 spectrometer (Palo Alto, CA). Chemical shifts were reported in the δ scale (ppm) by assigning the residual CD_2HCN solvent peak to 1.93 and 1.39 ppm for ^1H and ^{13}C , respectively. The two-dimensional ^1H - ^1H correlation spectroscopy (COSY) and rotating frame nuclear Overhauser enhancement spectroscopy (ROESY) spectra were acquired with a spectral width of 5397.4 Hz into 1K data points in f2, with 270 increments in the f1 dimension. Solvent suppression was carried out by presaturation. The mixing time for two-dimensional ^1H - ^1H ROESY was 0.3 s. The delays between successive pulses were 0.6 and 1.0 s for two-dimensional ^1H - ^1H COSY and ROESY, respectively.

In a separate set of experiments, NMR analysis was carried out on the synthetic standard of MK-0524 (1 mg) and its two major metabolites M2 and M8 (~50 μg based on radioactivity) isolated from the incubation of [^{14}C]MK-0524 in monkey hepatocytes. The ^1H and ^{13}C spectra were recorded as above. The two-dimensional ^1H - ^1H COSY and ROESY spectra were acquired with a spectral width of 4197.9 Hz into 1K data points in f2, with 419 increments in

the f1 dimension. Solvent suppression was carried out by presaturation. The mixing time for two-dimensional ^1H - ^1H ROESY was 0.3 s. The delays between successive pulses were 0.5 and 1.0 s for two-dimensional ^1H - ^1H COSY and ROESY, respectively. The two-dimensional ^1H - ^{13}C heteronuclear single quantum correlation experimental data were acquired with spectral widths of 4197.9 and 30,154.5 Hz for ^1H and ^{13}C dimensions, respectively, 1K data points in f2, and with 301 increments in f1 dimension. The 90° pulses were 5.35 and 12.0 μs for ^1H and ^{13}C , respectively. The delay during acquisition was 3.6 ms ($1/2 J_{\text{CH}}$).

Bioanalytical Methods. For the glucuronidation reactions, extracts of reaction mixtures were analyzed on a 3×50 mm Luna 3- μm Phenyl-Hexyl column (Phenomenex, Torrance, CA) with UV detection (Shimadzu LC10A system) at 311 nm. Mobile phase A consisted of 10 mM aqueous ammonium acetate containing 0.1% acetic acid, and mobile phase B consisted of acetonitrile/methanol (92.8:7.2, v/v) containing 7.2 mM ammonium acetate and 0.1% acetic acid. The separation of the acyl glucuronide, M2, from the parent compound was performed over 7.5 min using linear gradient elution from 35 to 95% B at a flow rate of 1 ml/min.

Turnover was calculated as the glucuronide peak area divided by the sum of glucuronide and parent peak areas. Both K_m and V_{max} parameters were calculated using Enzyme Kinetics! Pro software (ChemSW, Inc., Fairfield, CA) with the least-squares method and by fitting the data to the Michaelis-Menten equation. Metabolic profiles of [^{14}C]MK-0524 from microsomal and hepatocyte incubations were obtained using a 4.6×250 mm Zorbax 5- μm SB-Phenyl column (Agilent Technologies, Palo Alto, CA) with UV detection at 311 nm and monitoring the radioactive eluate using a β -RAM detector. Mobile phases were as above. The column was eluted over a 40-min period with a linear gradient from 25 to 65% B. All the HPLC separations were carried out at room temperature at a flow rate of 1 ml/min.

Metabolite identification was established by comparison to synthetic standards, where available, using retention time comparison and mass spectral data. LC/MS analysis was performed on a PerkinElmer (Boston, MA) Sciex API 2000 with Turbo-IonSpray in the negative ionization mode.

For metabolite identification from hepatocyte and microsomal incubations, LC/MS experiments were conducted using a Finnigan Deca XP ion trap mass spectrometer that was interfaced with a PerkinElmer autosampler (Series 200) and a Shimadzu HPLC system consisting of LC-10AD VP pumps, and a SCL-10A VP system controller. Both LC/MS and LC/MS² experiments were carried out using the electrospray interface operating in the negative ion mode. The source temperature was maintained at 300°C, and the spray voltage was 4500 V. For MS² experiments, relative collision energy of 35 eV was used. Data-dependent scans were used to assist in the detection of metabolites. A 4.6×250 -mm, 5- μm Zorbax RX-C18 column (Agilent Technologies, Wilmington, DE) was used for HPLC separation. The flow rate was 1 ml/min, and the LC effluent was split, with one-fourth directed into the mass spectrometer and the remainder into the radiometric detector (β -RAM). Mobile phase and gradient conditions were as used above. Identification of the acyl glucuronide metabolite M2, the monohydroxylated metabolites M1 and M4, and the keto-metabolite M3 were confirmed using authentic standards.

Results

Glucuronidation of MK-0524. The in vitro glucuronidation of MK-0524 was examined in liver microsomes from male Sprague-Dawley rat, beagle dog, cynomolgus monkey, and human (microsomes from mixed genders). Glucuronidation in human intestinal microsomes also was studied. The V_{max} , K_m , and intrinsic clearance (V_{max}/K_m) values are listed in Table 1. A species comparison of the in vitro intrinsic clearance values for the glucuronidation of MK-0524 in liver microsomes followed the rank order rat > monkey ~ dog > human and was 262, 100, 80, and 22 $\mu\text{l}/\text{min}/\text{mg}$, respectively. The intrinsic clearance in human intestinal microsomes was similar to that in human liver (~ 27 $\mu\text{l}/\text{min}/\text{mg}$).

The rates of glucuronidation of MK-0524 by different human UGT isoforms are depicted in Table 2. The data indicate that UGT1A3, UGT2B7, and UGT1A9 exhibited the highest rate of glucuronidation as a function of the amount of protein used in the incubations—413,

TABLE 1

Mean kinetic parameters for the glucuronidation of MK-0524 in microsomal preparations from rat, dog, cynomolgus monkey, human liver, and human intestine

MK-0524 (0.3–40 μM) was incubated with liver microsomes in the presence of 2 mM UDPGA at 37°C. Values represent mean; $n = 2$.

Species	V_{max}	K_m	V_{max}/K_m
	pmol/min/mg	μM	$\mu\text{l}/\text{min}/\text{mg}$
Rat liver	1872	7	262
Dog liver	1577	20	80
Cynomolgus monkey liver	1234	12	100
Human liver	425	19	22
Human intestine	184	7	27

TABLE 2

Mean apparent kinetic parameters for the glucuronidation of MK-0524 with recombinant human UGT

MK-0524 (0.3–40 μM) was incubated with membrane preparations of recombinant human UGT from baculovirus-infected cells (0.1 mg/ml) in the presence of 2 mM UDPGA at 37°C. Values represent mean; $n = 2$.

Human UGT Isoform	App V_{max}	App K_m	App V_{max}/K_m
	pmol/min/mg	μM	$\mu\text{l}/\text{min}/\text{mg}$
UGT1A1	8	1.9	4
UGT1A3	413	6.6	62
UGT1A8	N.D. ^a	N.D.	N.D.
UGT1A9	87	13.3	7
UGT1A10	N.D.	N.D.	N.D.
UGT2B7	106	3.3	32

^a N.D., not determined. No metabolite formation was observed.

106, and 87 pmol/min/mg, respectively. The rate of metabolism with UGT1A1 was lower than the other isoforms, 8 pmol/min/mg protein, whereas UGT1A8 and UGT1A10 did not exhibit any turnover of the compound. To determine the major UGT isoform(s) involved in the glucuronidation of MK-0524 in humans, the apparent K_m values in recombinant human UGT isoforms were determined and compared with those values obtained in human liver and intestinal microsomes. The K_m for UGT1A9 (13 μM) was similar to the K_m in human liver microsomes (19 μM), indicating that UGT1A9 was the isoform that most likely had the potential to catalyze the glucuronidation of MK-0524 in the liver. Also, 1-hydroxypyrene, an avid substrate for UGT1A9 (Luukkanen et al., 2001), was shown to inhibit the glucuronidation of MK-0524 in human liver microsomes by 92% at a concentration of 125 μM . The calculated IC₅₀ value was 27 μM (data not shown).

In the case of human intestine, the K_m for MK-0524 glucuronidation in human intestinal microsomal preparation, 7 μM , was similar to that estimated for UGT1A3 ($K_m = 6.6$ μM) and UGT2B7 ($K_m = 3.3$ μM), suggesting that both these isoforms may play a role in the glucuronidation of MK-0524 in the gut.

NADPH-Dependent Metabolism of MK-0524. The NADPH-dependent metabolism of [^{14}C]MK-0524 was investigated with liver microsomes from rat, beagle dog, rhesus monkey, and humans (metabolic pathway depicted in Fig. 1). The poor solubility of the parent compound in microsomal incubations precluded the estimation of definitive in vitro kinetic parameters. Nevertheless, the rate of phase I metabolism of MK-0524 with human liver microsomes was considerably slower than glucuronidation, as depicted in Fig. 2. Metabolites formed and radioactive metabolite profiles from liver microsomal incubations of MK-0524 (10 μM) were qualitatively similar across species and are shown in Table 3 and Fig. 3. Identification of major metabolites was based on comparison with standards, where available, and LC/MS/MS analysis (see below). The major oxidative metabolites

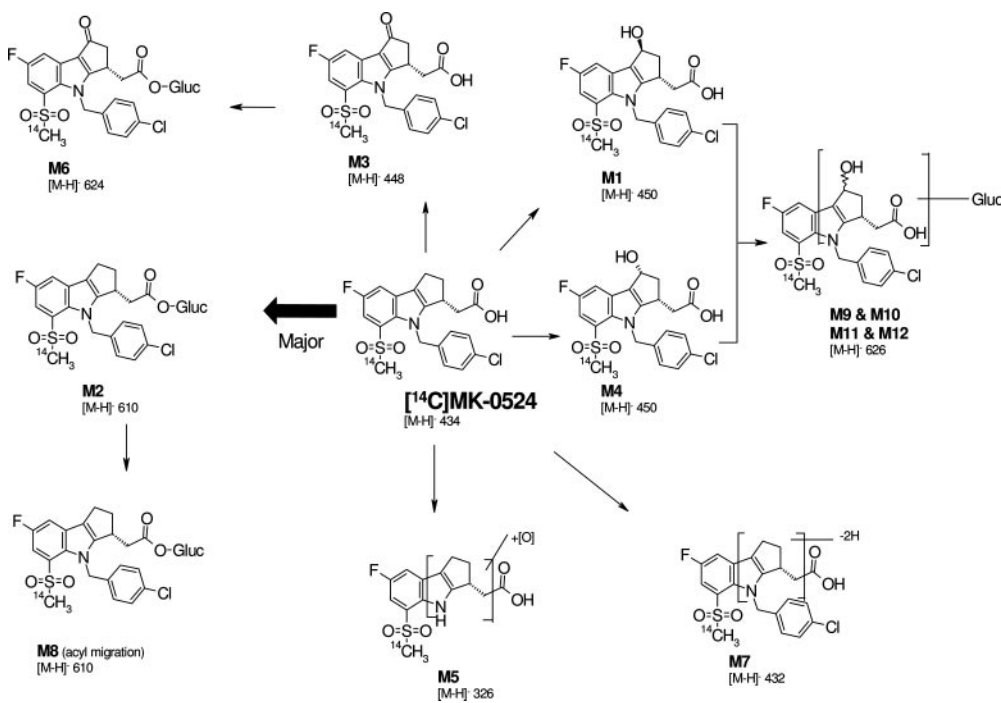


FIG. 1. Proposed metabolic pathways for MK-0524

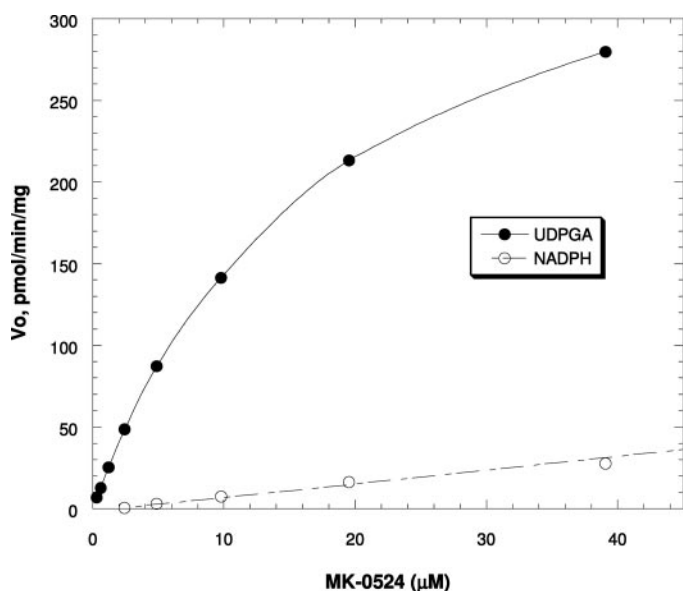


FIG. 2. Comparison of UDPGA- and NADPH-dependent metabolism of MK-0524 by human liver microsomes.

in all the species were the monohydroxylated epimers, M1 and M4. Trace amounts of the keto-metabolite, M3, were formed in rat, monkey, and human microsomes. Rat liver microsomes also generated minor amounts of an *N*-dealkylated metabolite of a monohydroxylated product, M5. An additional oxidized metabolite, M7, was present as a minor metabolite in all the species; however, the exact structure has not yet been identified. The major metabolites formed in human intestinal microsomes also were M1 and M4 (Fig. 4). The metabolism of MK-0524 was also studied in the presence of both NADPH and UDPGA in monkey liver microsomes (Fig. 5). The major metabolite was the acyl glucuronide, M2, along with glucuronides of M1, designated as M9 and M10. Also identified by mass spectrometry were minor amounts of the glucuronides of M4, designated as M11 or M12,

and a glucuronide of M3, M6, the structure of which was identified by NMR analysis (see below).

Incubations of MK-0524 with recombinant human P450s suggested the major involvement of CYP3A4, with a minor contribution from CYP2C9, in the formation of the two major phase I metabolites, M1 and M4 (Table 4; Fig. 6). The rates of formation of M1 by CYP3A4 and CYP2C9 were 19.2 and 1.9 pmol/pmol \cdot h, respectively. The rates of formation of M4 by CYP3A4 and CYP2C9 were 27 and 2.4 pmol/pmol \cdot h, respectively. There was negligible metabolism of MK-0524 by recombinant CYP1A1, CYP2A6, CYP2C19, CYP2D6, and CYP2E1 microsomes. The involvement of CYP3A4 and CYP2C9 was confirmed by conducting human liver microsomal incubations in the presence of monoclonal antibodies to these two P450s. At the highest concentration of antibody used (100 $\mu\text{l/mg}$ microsomal protein), approximately 85 and 15% of MK-0524 metabolism in human liver microsomes was inhibited by anti-CYP3A4 and anti-2C8/9 antibodies, respectively (Fig. 7). Incubation with a mixture of anti-CYP3A4 and anti-2C8/9 antibodies resulted in 98% inhibition of phase I metabolism of MK-0524.

Hepatocyte Incubations. After incubations of MK-0524 (10 μM) with Sprague-Dawley rat, beagle dog, rhesus monkey, and human cryopreserved hepatocyte suspensions, substantial turnover of the parent compound was observed, with qualitatively similar metabolite profiles across species. Identification of major metabolites was based on comparison with standards, where available, and LC/MS/MS analysis (see below). Representative metabolite profiles following a 4-h incubation are shown in Fig. 8. The major metabolites in all the species were M2, the acyl glucuronide of MK-0524, and its rearranged products. The latter metabolites were identified by NMR analysis (see below) to be a mixture of the stable α -anomer, M8, and at least one additional migration product. In addition, phase I metabolites, such as M1, M4, and M3, also were identified as minor entities in rat, monkey, and human hepatocytes. Glucuronic acid conjugates of M1, M4, and M3 also were detected in small amounts in these species and were designated as M9 or M10, M11 or M12, and M6, respectively (Table 3). Also present in small amounts in rat hepatocytes was

TABLE 3

Metabolites of MK-0524 detected in liver microsomes and hepatocytes

[¹⁴C]MK-0524 was incubated with liver microsomes (and an NADPH-regenerating system) and with hepatocytes. Acetonitrile supernatants of the incubations were analyzed by LC/MS and LC/MS/MS (see text for details).

Metabolite ^a	RT	[M-H] ⁻	MW	RLM	RH	DLM	DH	MLM	MH	HLM	HH
MK-0524	32.9	434	435	✓ ^b	✓	✓	✓	✓	✓	✓	✓
M1	20.6	450	451	✓	✓	✓	N.D.	✓	✓	✓	✓
M2	17.6	610	611	N.D.	✓	N.D.	✓	N.D.	✓	N.D.	✓
M3	23.1	448	449	✓	✓	N.D.	N.D.	✓	✓	✓	✓
M4	21.9	450	451	✓	✓	✓	N.D.	✓	✓	✓	✓
M5	10.4	326	327	✓	N.D.	N.D.	N.D.	✓	N.D.	N.D.	N.D.
M6	12.1	624	625	N.D.	✓	N.D.	N.D.	N.D.	✓	N.D.	✓
M7	31.3	432	433	✓	✓	✓	N.D.	✓	N.D.	✓	N.D.
M8	18.4	610	611	N.D.	✓	N.D.	✓	N.D.	✓	N.D.	✓
M9	10.7	626	627	N.D.	✓	N.D.	N.D.	N.D.	✓	N.D.	✓
M10	11.4	626	627	N.D.	✓	N.D.	N.D.	N.D.	✓	N.D.	✓
M11	12.9	626	627	N.D.	✓	N.D.	N.D.	N.D.	✓	N.D.	✓
M12	13.3	626	627	N.D.	✓	N.D.	N.D.	N.D.	✓	N.D.	✓

RT, retention time (min); [M-H]⁻, *m/z*; MW, molecular weight (amu); RLM, rat liver microsomes; RH, rat hepatocytes; DLM, dog liver microsomes; DH, dog hepatocytes; MLM, rhesus monkey liver microsomes; MH, rhesus monkey hepatocytes; HLM, human liver microsomes; HH, human hepatocytes; N.D., not detected.

^a See Fig. 1 for chemical structures.

^b ✓, detected.

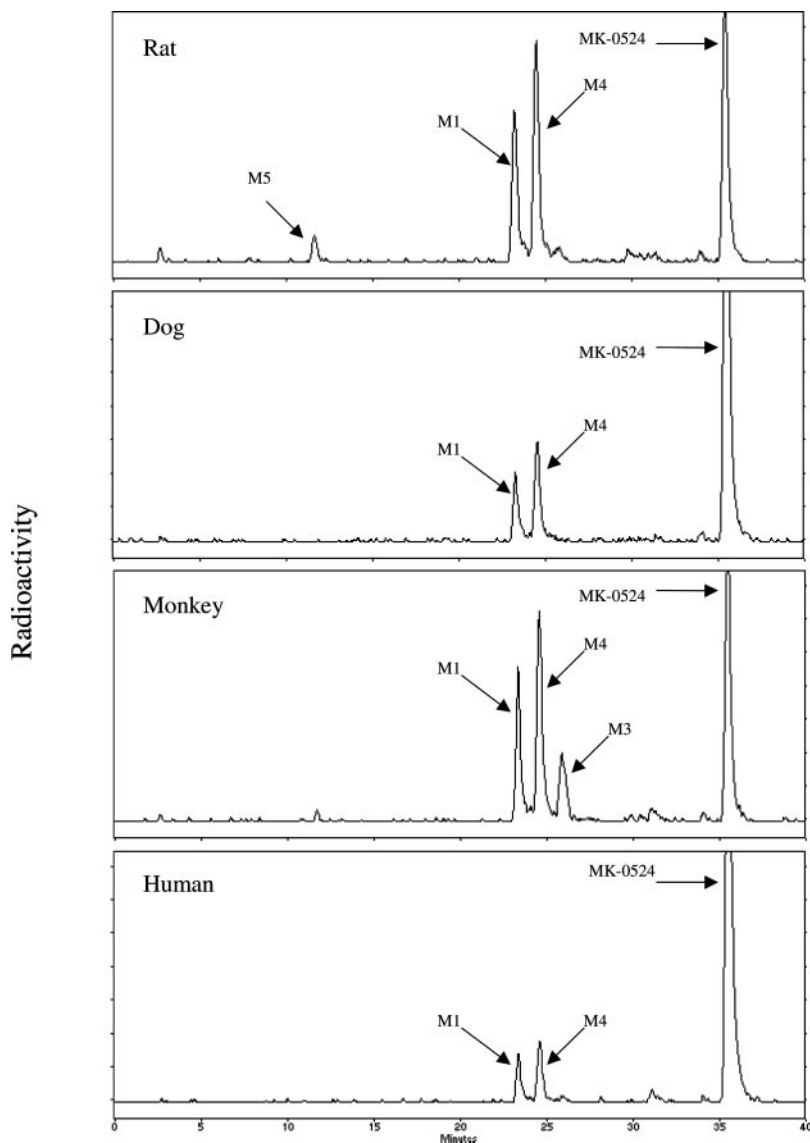


FIG. 3. Radiochromatograms illustrating the representative metabolite profiles of [¹⁴C]MK-0524 in incubations with NADPH-enriched male rat, dog, rhesus monkey, and human liver microsomes.

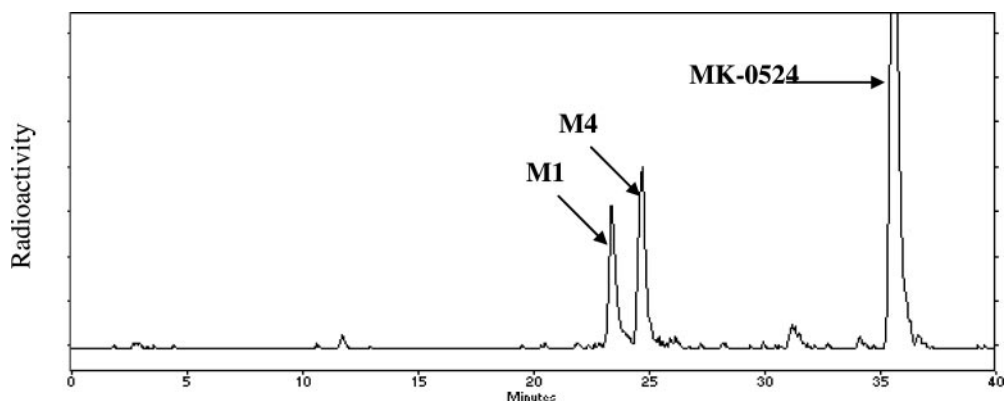


FIG. 4. Radiochromatograms illustrating metabolite profile of [^{14}C]MK-0524 incubations with NADPH-enriched male human intestinal microsomes.

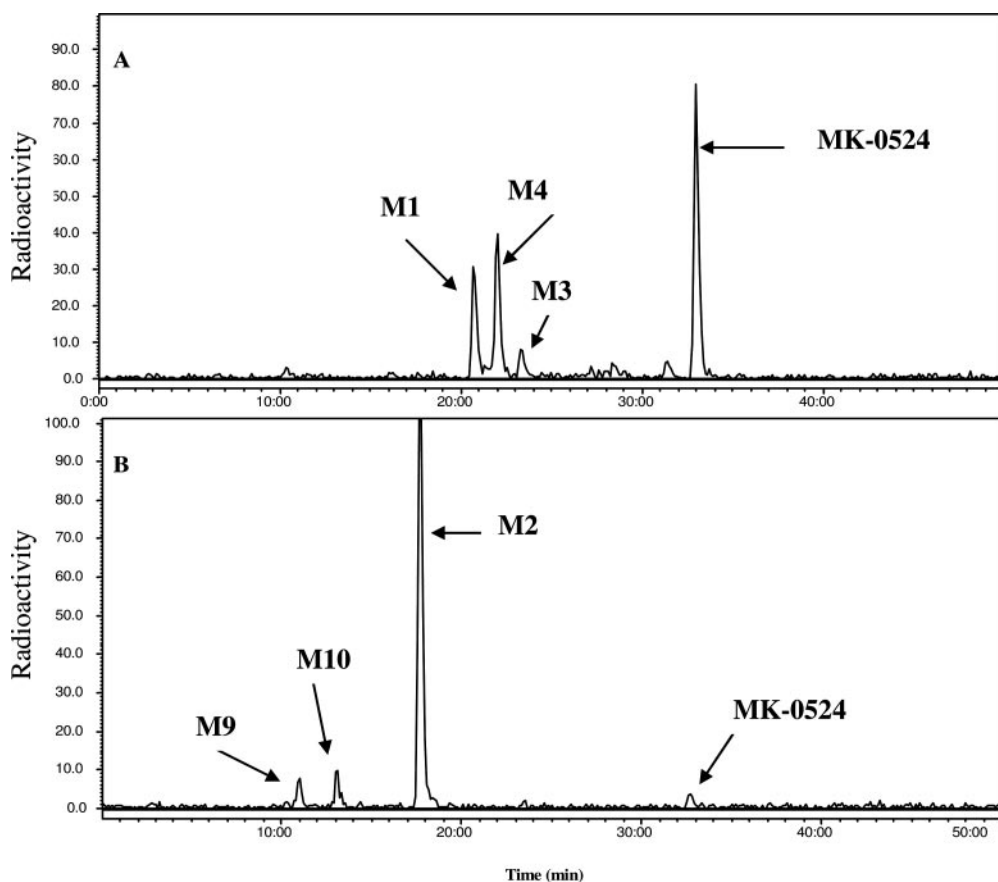


FIG. 5. Metabolism of [^{14}C] MK-0524 in NADPH-enriched rhesus monkey liver microsomes in the absence (A) or presence (B) of UDPGA.

M7 and M6, the glucuronide conjugate of M3 in rat, monkey, and human hepatocytes.

LC/MS/MS Analysis. The parent compound, MK-0524, gave a deprotonated molecular ion $[\text{M}-\text{H}]^-$ at m/z 434 (Fig. 9; Table 5). The collision-induced dissociation spectrum yielded fragment ions with m/z at 416 and 390, which corresponded to loss of water (18 Da) and carbon dioxide (44 Da) from the parent. Additionally, a fragment ion at m/z 278 corresponded to the loss of the chlorophenyl moiety from m/z 390.

The acyl glucuronide metabolite of the parent compound and its rearranged isomer, M2 and M8, respectively, gave deprotonated molecular ions $[\text{M}-\text{H}]^-$ at m/z 610, corresponding to an addition of 176 Da to the parent compound (m/z 434). Additional fragments were 434 (as a result of loss of m/z 176) and similar to those obtained from the parent compound (above), viz., m/z 278, 390, and 416 Da.

The hydroxylated epimers, M1 and M4, gave rise to deprotonated molecular ion $[\text{M}-\text{H}]^-$ at m/z of 450, indicative of the addition of 16

TABLE 4

Rates of formation of the monohydroxylated metabolites of MK-0524, M1 and M4, by recombinant human P450s

MK-0524 (10 μM) was incubated for 90 min with P450 microsomes (20 pmol P450) in the presence of NADPH at 37°C. Values represent mean; $n = 2$.

P450	M1 <i>pmol/pmol · h</i>	M4 <i>pmol/pmol · h</i>
CYP1A1	0.09	0.2
CYP2A6	N.D.	N.D.
CYP2C9	1.9	2.4
CYP2C19	N.D.	0.17
CYP2D6	N.D.	N.D.
CYP2E1	N.D.	N.D.
CYP3A4	19.2	27

N.D., not detected.

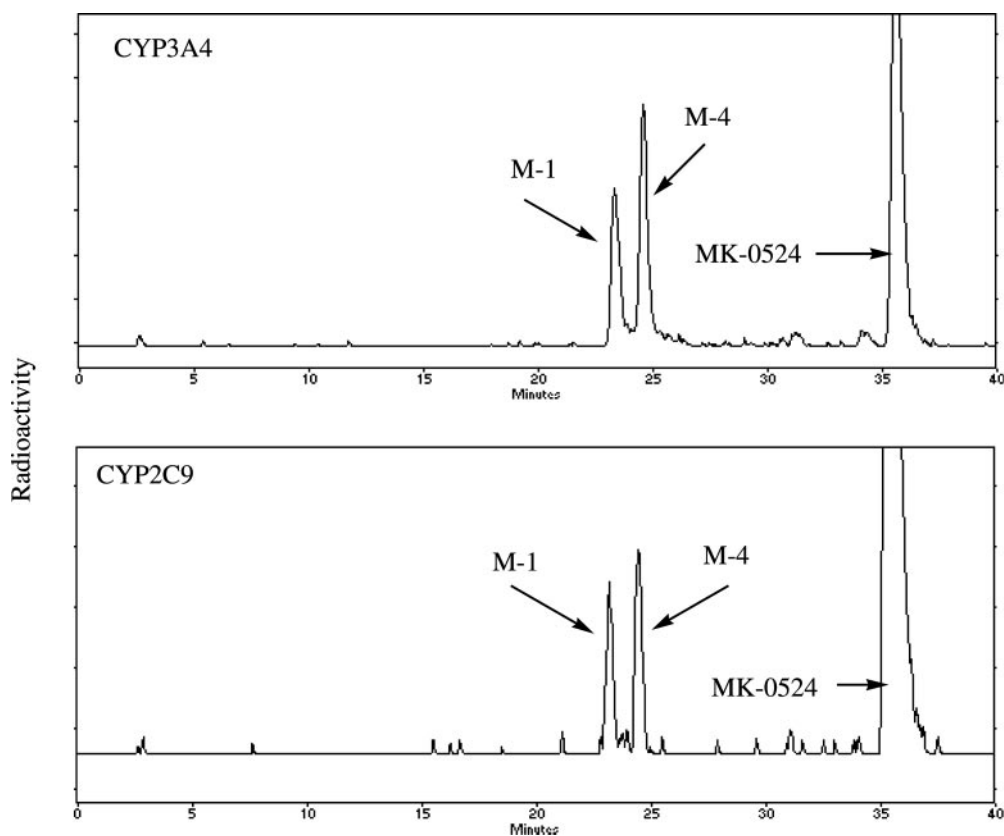


Fig. 6. Radiochromatograms illustrating the metabolite profiles of [^{14}C]MK-0524 incubations with recombinant human CYP3A4 and CYP2C9 in the presence of NADPH.

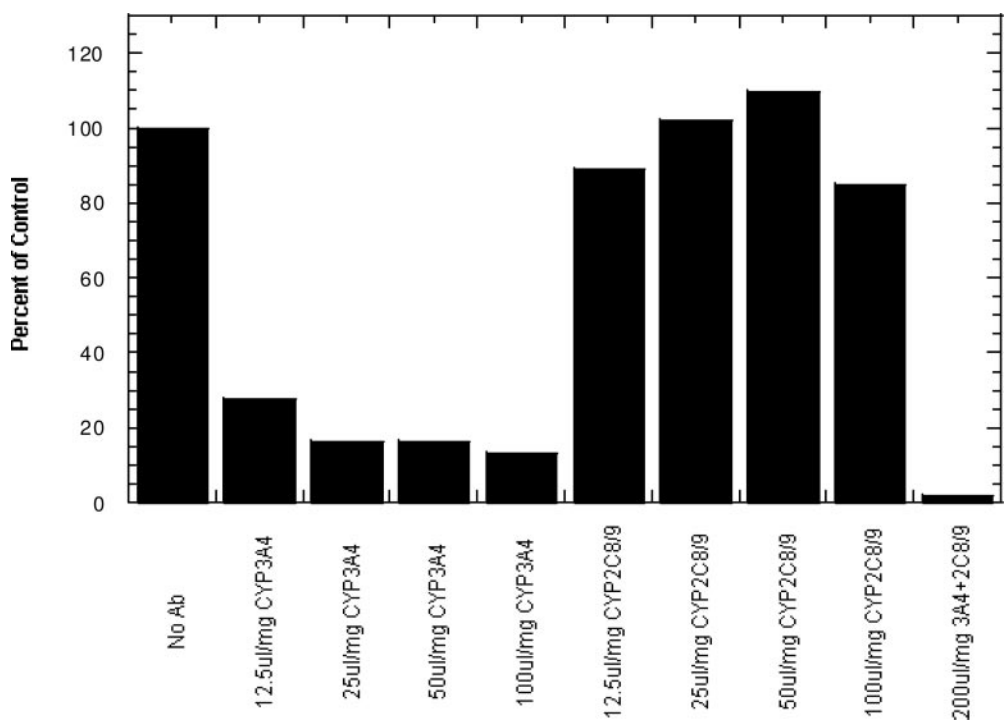


Fig. 7. Effect of anti-P450 monoclonal antibodies on the NADPH-dependent metabolism of [^{14}C]MK-0524 by human liver microsomes.

Da to the parent compound. Similar fragments as above, which corresponded to losses of water and carbon dioxide, were observed at m/z 432 and 406, respectively. Furthermore, a major fragment ion at m/z 388 indicative of loss of water (18 Da) from m/z 406 was indicative of hydroxylation of the cyclopentane ring.

The keto derivative (M3) gave rise to a deprotonated molecular ion $[\text{M}-\text{H}]^-$ at m/z 448, an addition of 14 Da on the parent compound,

indicating an oxidation at an aliphatic position followed by further oxidation to a carbonyl. The major product ions were m/z 430 (loss of water) and m/z 404 (loss of carbon dioxide). Also, a major fragment at m/z 376 corresponded to the loss of 28 Da (CO) from m/z 404 and was indicative of a keto group on the cyclopentane ring.

A minor metabolite, M5, was identified as the *N*-dealkylated derivative of a hydroxylated metabolite. It gave rise to a deprotonated

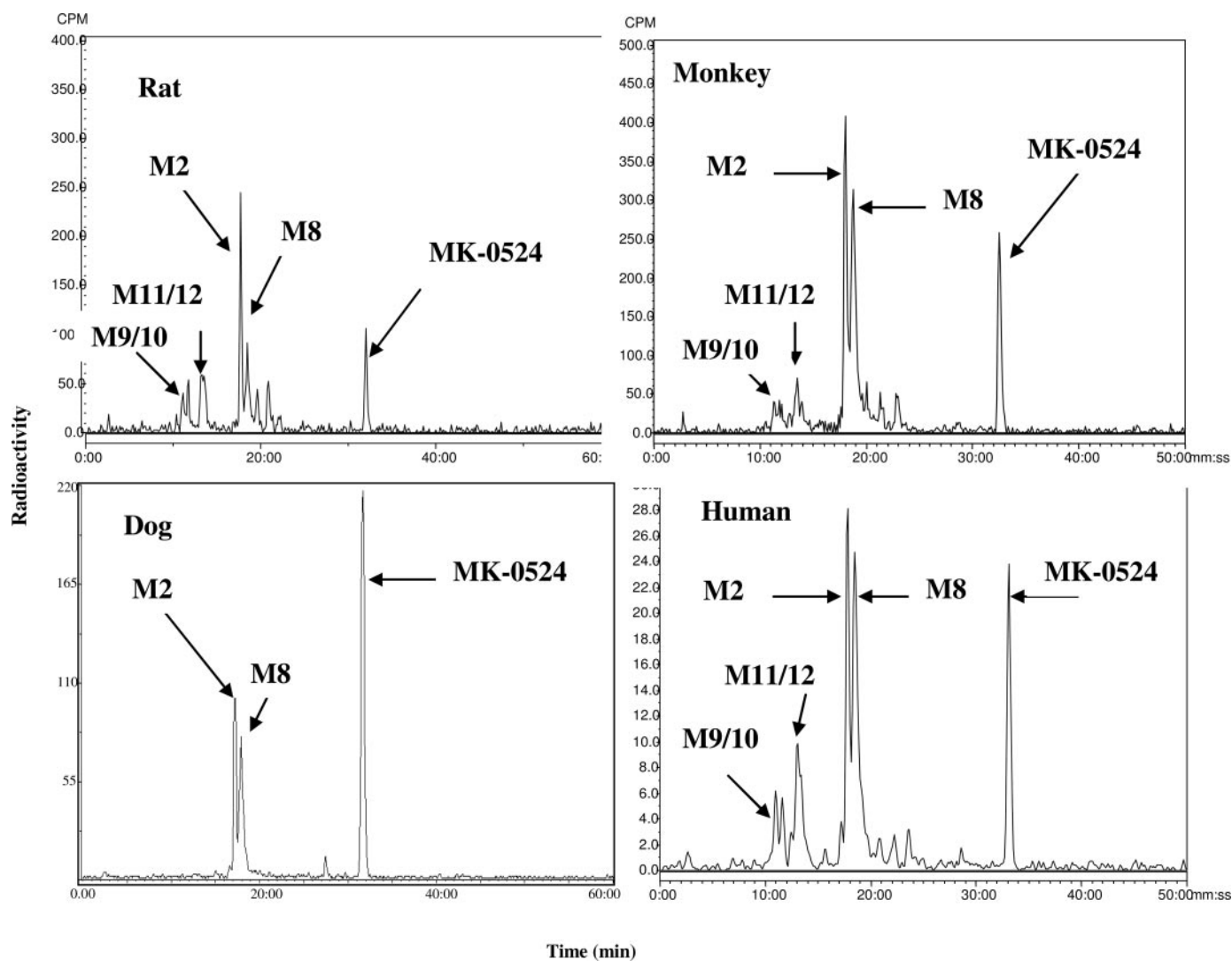


FIG. 8. Radiochromatograms illustrating the metabolism of $[^{14}\text{C}]$ MK-0524 in incubations with rat, dog, rhesus monkey, and human hepatocytes.

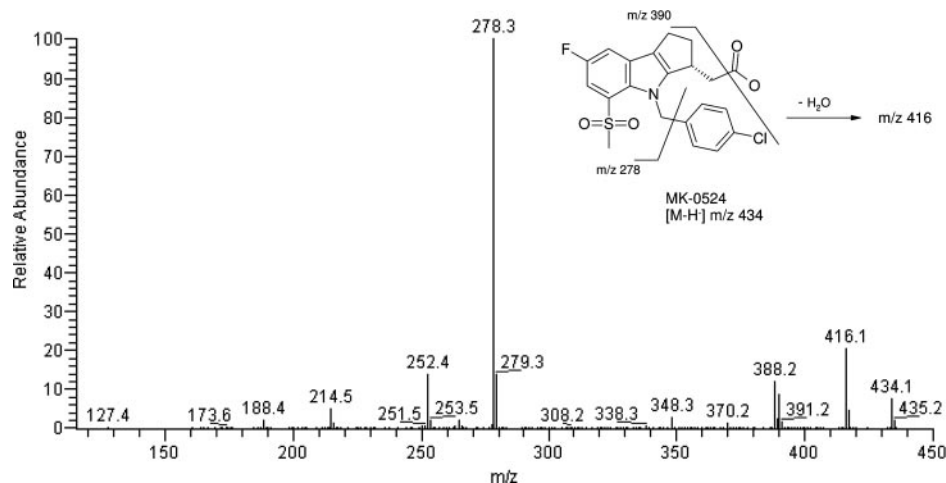


FIG. 9. MS/MS spectrum of MK-0524 and assignments of its fragment ions.

molecular ion $[M-H]^-$ at m/z 326, corresponding to a loss of 126 Da and addition of 16 Da to the mass of the parent compound. The collision-induced dissociation spectrum of this metabolite yielded fragments at m/z 308 and 282 [loss of water (18 Da) and carbon dioxide (44 Da), respectively]. Further loss of water from m/z 282

yielded a major fragment at m/z 264, indicative of an aliphatic hydroxyl group on the cyclopentane ring.

An oxidative metabolite, identified as M7, gave rise to a deprotonated molecular ion at m/z 432, corresponding to a loss of 2 Da from the parent molecule. The characteristic loss of carbon dioxide (44 Da)

TABLE 5
LC/MS/MS analysis of metabolites of MK-0524

Metabolite	<i>m/z</i>	Fragment Ions (<i>m/z</i>)
MK-0524	434	416, 390, 278
M1	450	432, 406, 388
M2	610	434, 416, 390, 278
M3	448	430, 404, 376
M4	450	432, 406, 388
M5	326	308, 282, 264
M7	432	388, 262
M9, M10, M11, M12	626	432, 406, 388

generated a major fragment at *m/z* 388. Also present was another fragment at *m/z* 262, formed as a result of the loss of the chloro-benzyl moiety (loss of 126 Da).

The acyl glucuronide conjugates of the hydroxylated metabolites (M9/M10 and M11/M12) were observed at *m/z* 626, corresponding to an addition of 176 Da to the mass of the hydroxylated metabolites M1 and M4 (*m/z* 450). Further fragments obtained were similar to those obtained with M1 and M4, viz., at *m/z* 432, 406, and 388.

NMR Identification. The structure of M2 (isolated from monkey liver microsomes fortified with UDPGA) was identified to be the acyl glucuronide of MK-0524, based on direct comparison of the proton ¹H NMR of the synthetic standard. M6 was isolated from the incubation of [¹⁴C]MK-0524 with monkey liver microsomes in the presence of NADPH and UDPGA. The ¹H NMR analysis suggests it to be the 1-β-*O*-acyl glucuronide of M3, based on the following observations: protons at position 1 are absent, suggesting oxidation to the ketone; the chemical shift (5.36 ppm) and coupling constant (8.1 Hz) of the anomeric proton indicate a 1-β-*O*-acyl glucuronide; and LC/MS data are consistent with the deprotonated molecular ion (*m/z* 624, [M + 176-H]) (data not shown).

Incubation of [¹⁴C]MK-0524 (50 μM) with monkey hepatocytes gave rise to two major chromatographic peaks (Fig. 8); both of these were identified as glucuronide conjugates of the parent compound by LC/MS (*m/z* 610, [M + 176-H]⁻, for both peaks). One of the peaks was identified as M2 by direct NMR comparison with the standard. The ¹H NMR of the second peak, designated as M8, indicated a mixture of two major components. COSY, ROESY, and heteronuclear single quantum correlation experiments were carried out to establish whether the components of that peak represented the acyl migration products derived from M2 (data not shown). One of the components of M8 was identified as an α-anomer based on the small coupling constant of the anomeric proton (5.18 ppm, 1H, J = 3.7 Hz). Because of extensive signal overlap, however, the anomeric stereochemistry of the second component was not determined (4.52–4.58 ppm) (data not shown).

Discussion

MK-0524, a novel DP1 antagonist that is under development for the treatment of niacin-induced flushing, was found to undergo extensive glucuronidation in hepatocytes and liver microsomes from preclinical species and humans. The rate of formation of the acyl glucuronide in microsomes was highest in the rat, followed by the monkey and dog, and then human intestine and liver. MK-0524 would be expected to undergo first-pass metabolism in the gut based on the propensity of the compound to undergo glucuronidation in vitro in human intestinal microsome preparations. Results from this article complement the results of the studies conducted to evaluate the in vivo metabolism of MK-0524 in preclinical species, wherein it was observed that the major route of elimination of the compound is via glucuronidation (Chang et al., 2006). Based on a comparison of the *K_m* values

generated in vitro using recombinant UGTs, UGT1A9 has the potential to catalyze the glucuronidation of MK-0524 in the human liver, and UGT1A3 and UGT2B7 have the potential to catalyze the glucuronidation in the human intestine. These three isoforms also exhibited higher rates of glucuronidation than those observed with UGT1A1, UGT1A8, and UGT1A10. However, comparison of the *V_{max}* values across these isoforms is not possible because accurate measurements of the UGT protein expression levels cannot be determined.

Glucuronidation is a principal step in the metabolic pathway for a wide variety of endogenous substrates and xenobiotics. Substrate specificities for UGTs are, however, broad and overlapping with several UGTs responsible for catalyzing specific reactions. However, some substrates have been shown to be selectively catalyzed by specific isoforms. Some examples of some of these are bilirubin, which is glucuronidated selectively by UGT1A1 (Bosma et al., 1994), propofol by UGT1A9 (Burchell et al., 1995), and morphine 6 glucuronidation by UGT2B7 (Coffman et al., 1997). In the case of compounds such as MK-0524, wherein several recombinant UGT isoforms are involved, a comparison of kinetic parameters determined using expressed protein with those determined in human liver microsomal preparations is probably the best method to evaluate substrate specificity (Remmel and Burchell, 1993). These determinations would probably be much more refined when specific monoclonal antibodies to specific human UGT isoforms become available. Many carboxylic acid-containing drugs, such as the nonsteroidal anti-inflammatory drugs clofibrac acid and valproic acid, are glucuronidated by UGT2B7, which is a major isoform present in the liver and gut tissue (Jin et al., 1993; King et al., 2001). The data obtained with MK-0524 glucuronidation are consistent with the involvement of UGT2B7 being the primary UGT isoform in the gut, based on the similarity of the *K_m* values for its glucuronidation in human gut preparation versus recombinant UGT2B7, 7 versus 3 μM, respectively.

MK-0524 was also susceptible to phase I metabolism in liver microsomes from preclinical species and humans; however, the extent was much lower than glucuronidation. The metabolism of MK-0524 was qualitatively similar in liver microsomes in preclinical species and humans. The major metabolites generated in all the species were the monohydroxylated epimers, M1 and M4. Smaller amounts of the keto- metabolite, M3, were also formed in all the species. Using recombinant P450s and monoclonal antibodies, it was concluded that the human P450s involved in the phase I metabolism of MK-0524 were CYP3A4 and CYP2C9.

The major metabolites of MK-0524 in hepatocyte preparations from the rat, dog, monkey, and humans were M2 (the acyl glucuronide of MK-0524), its α-anomer (M8), and other products of acyl migration. The phase I metabolites, M1, M3, M4, and their respective acyl glucuronides, were observed in trace amounts.

Overall, the in vitro metabolism of MK-0524 proceeded largely via glucuronidation.

Acknowledgments. We thank Dr. Deborah Nicoll-Griffith, Yves Aubin, Claudio Sturino, and other members of the Medicinal Chemistry Department of Merck Frosst for supplying the standards for M1, M3, and M4.

References

- Bosma PJ, Seppen J, Goldhoorn B, Bakker C, Oude Elferink RP, Chowdhury JR, Chowdhury NR, and Jansen PL (1994) Bilirubin UDP-glucuronosyltransferase 1 is the only relevant bilirubin glucuronidating isoform in man. *J Biol Chem* **269**:17960–17964.
- Burchell B, Brierley CH, and Rance D (1995) Specificity of human UDP-glucuronosyltransferases and xenobiotic glucuronidation. *Life Sci* **57**:1819–1831.
- Chang S, Reddy V, Pereira T, Dean B, Franklin R, and Karanam B (2006) The pharmacokinetics and disposition of MK-0524 a DP1 antagonist, in rats, dogs and monkeys. *Xenobiotica*, in press.
- Cheng K, Wu T-J, Wu KK, Sturino C, Metters K, Gottesdiener K, Wright SD, Wang Z, O'Neill

- G, Lai E, et al. (2006) Antagonism of the prostaglandin D2 receptor 1 suppresses nicotinic acid-induced vasodilation in mice and humans. *Proc Natl Acad Sci USA* **103**:6682–6687.
- Coffman BL, Rios GR, King CD, and Tephly TR (1997) Human UGT2B7 catalyzes morphine glucuronidation. *Drug Metab Dispos* **25**:1–4.
- Eklund B, Kaijser L, Nowak J, and Wennmalm A (1979) Prostaglandins contribute to the vasodilation induced by nicotinic acid. *Prostaglandins* **17**:821–830.
- Gentile S, Rubba P, Persico M, Bronzino P, Marmo R, and Faccenda F (1985) Improvement of the nicotinic acid test in the diagnosis of Gilbert's syndrome by pretreatment with indomethacin. *Hepatogastroenterology* **32**:267–269.
- Jin C, Miners JO, Lillywhite KJ, and Mackenzie PI (1993) Complementary deoxyribonucleic acid cloning and expression of a human liver uridine diphosphate-glucuronosyltransferase glucuronidating carboxylic acid-containing drugs. *J Pharmacol Exp Ther* **264**:475–479.
- King C, Tang W, Ngui J, Tephly T, and Braun M (2001) Characterization of rat and human UDP-glucuronosyltransferases responsible for the in vitro glucuronidation of diclofenac. *Toxicol Sci* **61**:49–53.
- Knoop RH (1999) Drug treatment of lipid disorders. *N Engl J Med* **341**:498–511.
- Luukkanen L, Mikkola J, Forsman T, Taavitsainen P, and Elovaara E (2001) Glucuronidation of 1-hydroxypyrene by human liver microsomes and human UDP-glucuronosyltransferases UGT1A6, UGT1A7, and UGT1A9: development of a high-sensitivity glucuronidation assay for human tissue. *Drug Metab Dispos* **29**:1096–1101.
- Morrow JD, Awad JA, Oates JA, Roberts LJ 2nd (1992) Identification of skin as a major site of prostaglandin D2 release following oral administration of niacin in humans. *J Investig Dermatol* **98**:812–815.
- Nicoll-Griffith DA, Seto C, Aubin Y, Lévesque J-F, Chauret N, Day S, Silva JM, Trimble LA, Truchon JF, Bertelette C, et al. (2006) In vitro biotransformations of the prostaglandin D2 (DP) antagonist MK-0524 and synthesis of metabolites. *Bioorg Med Chem Lett* *in press*. *AL get(this, 'jour', 'Bioorg Med Chem Lett.');*, in press.
- Remmel RP and Burchell B (1993) Validation and use of cloned, expressed human drug metabolizing enzymes in heterologous cells for analysis of drug metabolism and drug-drug interactions. *Biochem Pharmacol* **46**:559–566.
- Rubenfire M (2004) Safety and compliance with once-daily niacin extended-release/lovastatin as initial therapy in the impact of medical subspecialty on patient compliance to treatment (IMPACT) study. *Am J Cardiol* **94**:306–311.
- Shepherd J, Packard DJ, Patsch JR, Gotto AM Jr, and Taunton OD (1979) Effects of nicotinic acid therapy on plasma high density lipoprotein subfraction distribution and composition and on apolipoprotein A metabolism. *J Clin Invest* **63**:858–867.
- Sturino CF, O'Neill G, Lachance N, Boyd M, Berthelette C, Labelle M, Li L, Roy B, Scheiget J, Tsou N, et al. (2006) Discovery of a potent and selective PGD₂ receptor antagonist [(3R)-4-(4-chlorobenzyl)-7-fluoro-5-(methylsulfonyl)-1,2,3,4-tetrahydrocyclopenta[b]indol-3-yl]-acetic acid (MK-0524). *J Med Chem*, in press.
- Vogt A, Kassner U, Hostalek U, and Steinhagen-Thiessen E (2006) On behalf of the Nautilus Study Group, 2006. Evaluation of safety and tolerability of prolonged-release nicotinic acid in a usual care setting. *Curr Med Res Opin* **22**:417–425.
- Zhao X-Q, Morse JS, Dowdy AA, Heise N, DeAngelis D, Frohlich J, Chait A, Albers JJ, and Brown BG (2004) Safety and tolerability of simvastatin plus niacin in patients with coronary artery disease and low high-density lipoprotein cholesterol (The HDL Atherosclerosis Treatment Study). *Am J Cardiol* **93**:307–312.

Address correspondence to: Bindhu Karanam, Merck Research Laboratories, Department of Drug Metabolism, RY80E-200, P.O. Box 2000, Rahway, NJ 07065. E-mail: bindhu_karanam@merck.com
